MODEL PREDICTIVE CONTROL FOR TRACKING OF REPETITIVE ORGAN MOTIONS DURING TELEOPERATED LAPAROSCOPIC INTERVENTIONS

R. Ginhoux[*], J. A. Gangloff[*], M. F. de Mathelin[*], L. Soler[†], J. Leroy[†], J. Marescaux[†]

[*] LSIIT UMR 7005 CNRS — Strasbourg I University, Bd. S. Brant, BP 10413, F-67412 Illkirch Cédex, France
e-mail: {ginhoux,gangloff,demath}@eavr.u-strasbg.fr

[†] IRCAD/EITS — University Hospital of Strasbourg, 1, Place de l'Hôpital, F-67000 Strasbourg, France

Keywords: unconstrained generalized predictive control, periodic disturbance rejection, repetitive control, surgical robotics, visual servoing.

Abstract

Periodic deformations of organs which are due to respiratory movements may be critical disturbances for surgeons manipulating robotic control systems during laparoscopic interventions or tele-surgery. Indeed, the surgeon has to manually compensate for these motions if accurate gestures are needed, like, *e.g.*, during suturing. This paper proposes a repetitive model predictive control scheme for driving a surgical robot towards the reference trajectory defined by the surgeon, while tracking periodic disturbances of known periods on the output. A new cost function is developed for an unconstrained generalized predictive control scheme based on a repetitive multiple input-output model of the robot. Contributions of the controller output to reference tracking and to disturbance rejection are split and computed separately; then, filtering of repetitive disturbances and tracking of the reference trajectory can be independently weighted by the controller while simultaneously running on the plant. The proposed control scheme is validated through simulations and experimental results shown in a surgical robotics application.

1 Introduction

The rejection of periodic disturbances is a common problem in control applications where the period of the disturbance is assumed to be known. Repetitive control is often considered as it makes use of the internal model principle to generate a periodic control signal, thereby enabling asymptotic rejection of the disturbance. Moreover, the control scheme may well benefit from the use of ideas from model predictive control: by combining the model of the perturbation — that is, a periodic signal generator — with a model of the plant, one can get the plant output anticipate future disturbances.

Several applications of Model Predictive Control (MPC) to the rejection of periodic disturbances can be found in the litterature: a dynamic model describing the oscillatory behavior of a chemical process is shown in [7], a mixture of repetitive control and predictive control is found in [5] (for a chemical application too). These controllers are developped using the state-space formulation of MPC and linear time-invariant or even time-varying (as in [4]) descriptions of the plants; applications shown consider steady-state control where no distinction is made between a periodic output disturbance or a periodically varying reference.

In this paper, we consider the problem of a periodic disturbance due to respiratory movements in robotized laparoscopic surgery. Surgeons manipulating robotic systems during teleoperated interventions encounter critical disturbances due to these movements when the aim is to do precise tasks, like, *e.g.*, suturing. Repetitive organ motions actually have to be manually compensated for by the operator while he or she is driving the robotic arms through the teleoperation human interface. Therefore, the robotic plant has to follow the time-varying, non-periodic reference defined by the surgeon while also tracking the periodic disturbance of the organ motion.

To solve this problem, we define a multiple input-output MIMO model in the ARIMAX form that includes a repetitive noise model and derive a Repetitive Generalized Predictive Control (R-GPC) scheme. A new cost function is written where the controller outputs are split into two independent components, the first one depending only on the reference trajectory tracking for telemanipulation, the second one depending only on disturbance rejection on the output. Thanks to this separation, it is ensured that reference tracking and disturbance rejection are independent, and that they can be weighted separately; moreover, a real-time monitoring of both control outputs would prevent the system from saturating, thereby ensuring a safe teleoperation. The proposed control algorithm is validated on both simulated and *in-vivo* surgical conditions using a visual servoing application in robotized laparoscopic surgery.

The paper is organized as follows. The next section details the derivation of the R-GPC cost function that leads to separate control outputs. A token example is shown to demonstrate the controller behaviour on a 2-input 2-output plant with a periodic disturbance of known frequency. Section 3 discusses the application of the controller to the cancellation of breathing induced motions in robotized laparoscopic surgery. The control scheme is tested on a laboratory test-bed with use of an endoscopy-training box and in *in-vivo* conditions on a living pig.

2 Repetitive Generalized Predictive Control

This section derives an unconstrained Generalized Predictive Control (GPC) scheme based on a repetitive model of the system to be controlled. The plant is supposed to have multiple inputs and multiple outputs. Separate contributions of the control input to reference trajectory tracking and disturbance rejection are computed by means of a new cost function that ensures no interaction between both components.

2.1 Repetitive ARIMAX model

Unconstrained GPC was originally introduced by [2], where the system model is represented by an ARIMAX equation,

$$A(q^{-1})y(t) = B(q^{-1})u(t-1) + \frac{C(q^{-1})}{\Delta(q^{-1})}\,\xi(t) \tag{1}$$

where q^{-1} is the backward operator and $T_e = 1\,s$ is the (normalized) sampling period. We consider the MIMO case, where the plant has m inputs and n outputs: A, B and C are matrices of polynomials of respective sizes $n \times n$, $n \times m$ and $n \times n$. A and B model the system dynamics (polynomials in B may also include pure delays). ξ(t) is a vector of n independent zero-mean white noises that are colored by matrix C. Hereinafter we suppose matrix C is diagonal with each term on the diagonal equal to a polynomial c, $C = c\,I_{n\times n}$. Polynomial Δ is used to make noise ξ/Δ be non-stationary, which is suitable to model any perturbation in a control loop [1]. In this paper, we propose to include repetitive disturbances in the ARIMAX model by writing Δ as:

$$\Delta(q^{-1}) = \delta(q^{-1})\,\Delta_R(q^{-1}) \tag{2}$$
$$\text{with } \delta(q^{-1}) \triangleq 1 - q^{-1} \text{and } \Delta_R(q^{-1}) \triangleq 1 - q^{-T}$$

and $T \in \mathbb{N}$, $T \geq 2$, is the number of sampling periods in one period T^* of the disturbance. The perturbation model ξ/Δ is actually made periodic with a period equal to T. Including the periodic signal generator $\Delta_R(q^{-1})$ [6] in the plant model will then lead to a repetitive model predictive controller.

In the next section, we propose to split the control input into two terms so that they can be filtered independently.

2.2 Separation of control input

Writing $y(t)$ in Equation (1) as

$$y(t) = y_{\mathtt{th}}(t) + \epsilon(t) \tag{3}$$

is equivalent to the two following equations:

$$A\,y_{\mathtt{th}}(t) = B\,u_1(t-1) \tag{4}$$

$$A\,\epsilon(t) = B\,u_2(t-1) + \frac{C}{\Delta}\,\xi(t) \tag{5}$$

where $u(t)$ is now written as $u(t) = u_1(t) + u_2(t)$. Command $u_1(t)$ is the control input to the theoritical system model (4), leading to output measurement $y_{\mathtt{th}}(t)$. Command $u_2(t)$ is responsible for the actual plant to exhibit measurement error $\epsilon(t)$ when subject to noise and disturbances in the measurement signal.

By multiplying Equation (4) by δ it comes:

$$A\,\delta y_{\mathtt{th}}(t) = B\,\delta u_1(t-1) \tag{6}$$

Multiply Equation (5) by Δ and let A_R substitute for $\Delta_R A$ and B_R for $\Delta_R B$; we get:

$$A_R\,\delta\epsilon(t) = B_R\delta u_2(t-1) + C\,\xi(t) \tag{7}$$

Equations (6) and (7) provide two independent equations for computing increments of the theoritical output $y_{\mathtt{th}}(t)$ and the measurement error $\epsilon(t)$ from increments of control outputs $u_1(t-1)$ and $u_2(t-1)$. Equations (6) and (7) are used to derive optimal predictions $\hat{y}_{\mathtt{th}}(t+j)$ and $\hat{\epsilon}(t+j)$ of the two components of the system output at time $t+j$, which lead to the expression of the cost function in the next section. Details are left to the careful reader (see [1]).

2.3 Cost function

The cost function for the unconstrained R-GPC is defined as follows:

$$\begin{aligned}\mathcal{J}(u = u_1 + u_2, t) = &\sum_{j=N_1}^{N_2} \|\hat{y}_{\mathtt{th}}(t+j) - r(t+j)\|^2 \\ &+ \sum_{j=N_1}^{N_2} \|\hat{\epsilon}(t+j)\|^2 + \lambda \sum_{j=1}^{N_u} \|\delta u_1\,(t+j-1)\,\|^2 \\ &+ \mu \sum_{j=1}^{N_u} \|\delta u_2\,(t+j-1)\,\|^2 \end{aligned} \tag{8}$$

N_1, N_2 are respectively, the lower and upper bound of the cost horizon, and N_u is the length of the control cost horizon; $N_u < N_2$ and $\delta u_i(t+j-1) = 0$ for $j > N_u$, $i = 1$ or 2; λ and μ weight the relative importance of both control energies. The reference trajectory is denoted by $r(t)$. The aim is to compute the N_u future control increments $\delta u_1(t+j-1)$ so that the error between the predictions of the theoritical model outputs and the future references $r(t+j)$ is minimized; and the control increments $\delta u_2(t+j-1)$ so as to drive the actual system outputs towards the theoritical ones, or, equivalently, to compensate for the measurement disturbances. Note that the two sets of control increments separately contribute to the minimization of the cost function.

Advantage of this decomposition is manifold: the commands responsible for the cancellation of the perturbation can be filtered separately from the commands acting on the reference tracking; this means that low-pass filters or even nonlinear filters can increase the robustness against errors in the system model or measurement noise; different levels of saturation can be put on both control inputs in order to prevent teleoperated component $u_1(t)$ from saturating with no influence on the perturbation cancellation in case of large changes in the reference signal.

2.4 Derivation of the optimal solution

We now compute $u(t) = u_1(t) + u_2(t)$ that minimizes the cost function (8). The least square value of $\mathcal{J}$ is found with respect to $(\delta U_1,\ \delta U_2)$ as $(\delta U_1^*,\ \delta U_2^*)$ where:

$$\left\{ \begin{array}{rcl} \delta U_1^* & = & (G_1^\top G_1 + \lambda I)^{-1} G_1^\top (R - L_1) = K_1 (R - L_1) \\ \delta U_2^* & = & -(G_2^\top G_2 + \mu I)^{-1} G_2^\top L_2 = -K_2 L_2 \end{array} \right. \tag{9}$$

being $\delta U_1 \in \mathbb{R}^{N_u\, m}$ (resp. $\delta U_2 \in \mathbb{R}^{N_u\, m}$) the vector of u_1 (resp. u_2) increments:

$$\begin{array}{rcl} \delta U_1 & = & [\delta u_1(t), \delta u_1(t+1), ..., \delta u_1(t+N_u-1)]^T \\ \delta U_2 & = & [\delta u_2(t), \delta u_2(t+1), ..., \delta u_2(t+N_u-1)]^T; \end{array}$$

Matrices $K_1 \in \mathbb{R}^{N_u\, m \times (N_2 - N_1 + 1)n}$ and $K_2 \in \mathbb{R}^{N_u\, m \times (N_2 - N_1 + 1)n}$ are the two optimal gain matrices for the R-GPC controller. According to the receding horizon strategy [1], only the first value $\delta u_1(t)^*$ and $\delta u_2(t)^*$ of δU_1^* and δU_2^* in System (9) are used for computing $u(t) = u_1(t) + u_2(t)$ as

$$\left\{ \begin{array}{rcl} u_1(t) & = & \delta u_1(t)^* + u_1(t-1) \\ u_2(t) & = & \delta u_2(t)^* + u_2(t-1) \end{array} \right.$$

Therefore the only first lines of matrices K_1 and K_2 are actually considered by the controller in order to perform minimization of $\mathcal{J}$ at each time step.

2.5 A simple example

In this section we provide curves to demonstrate the controller behaviour on a token example (borrowed from [1]).

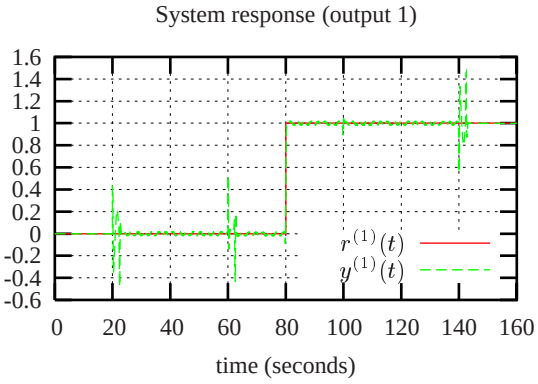

Figure 2: A simple example: System output and reference for output 1.

The plant model is the following:

$$\begin{pmatrix} y^{(1)}(z) \\ y^{(2)}(z) \end{pmatrix} = z^{-d} \begin{pmatrix} \frac{0.042 z^{-1}}{1-0.958 z^{-1}} & \frac{0.4758 z^{-1}}{1-0.9048 z^{-1}} \\ \frac{0.0582 z^{-1}}{1-0.9418 z^{-1}} & \frac{0.1445 z^{-1}}{1-0.9277 z^{-1}} \end{pmatrix} \begin{pmatrix} u^{(1)}(z) \\ u^{(2)}(z) \end{pmatrix}$$

where $d = 3$ is the plant's pure delay. The sampling period is $T_e = 0.040\, s$. The plant is submitted to a sinusoidal disturbance with period $T^* = 2.4\, s$ and amplitude 0.5 on its both outputs from $t = 20\, s$ to $t = 140\, s$; we also add a constant disturbance step of amplitude 0.5 from $t = 60\, s$ to the end. The reference trajectory is a unit step arriving at $t = 80\, s$ for input 1 and $t = 100\, s$ for input 2.

Polynomial C is chosen as $C = 1 - 0.999 z^{-1}$. The true period T^* of the sinusoidal disturbance is known by the controller and polynomial Δ is taken as $\Delta = (1 - q^{-1})(1 - q^{-\lfloor T^*/T_e \rfloor})$. The other R-GPC parameters are chosen as: $N_1 = 8;\ N_2 = 45;\ N_u = 30;\ \lambda = 0.5;\ \mu = 0.6;$

Figure 2,3 depict the time evolution of both plant outputs showing reference step tracking and constant and periodic disturbance rejection. A transient appears at $t = 20\, s$ and $t = 140\, s$ that corresponds to start/end of the sinus; the transient at $t = 60\, s$ refers to the rejection of the constant disturbance.

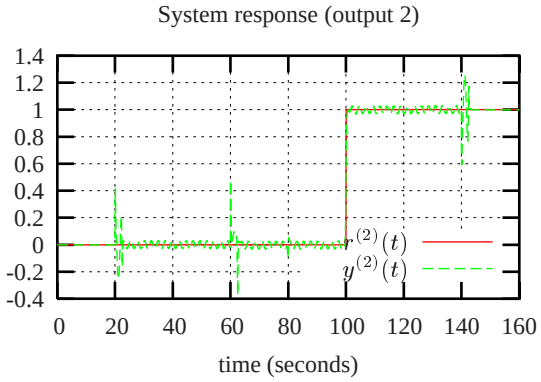

Figure 3: A simple example: System output and reference for output 2.

With curves in Figure 1, one can verify there is no coupling between the two control parts $u_1^{(1)}(t)$ and $u_2^{(1)}(t)$ of controller output 1. Similar curves are obtained for controller output 2. Components $u_1^{(i)}(t)$ only depend on the trajectory to be followed by the plant; components $u_2^{(i)}(t)$ are generated due to disturbances on the plant outputs and are not influenced by the trajectory tracking ($i = 1,\ 2$).

3 Cancellation of Breathing-Induced Motions in Robotized Laparoscopic Surgery

The controller is now applied to the cancellation of breathing induced motions in robotized laparoscopic surgery. The robot used is an AESOP® laparoscopic arm (Computer Motion, Inc.) shown in Figs. 4, 5.

We address the problem of keeping constant the distance from the tip of the instrument to the moving organ's surface (*i.e.*, the instrument's depth), as it is viewed from a fixed endoscope (see Figure 5b). The technique used for distance estimation in endoscopic images is based on a laser pointing instrument and is described in [3]. As a consequence, the robot is modelled as a single-input single-output plant. We consider only the dy-

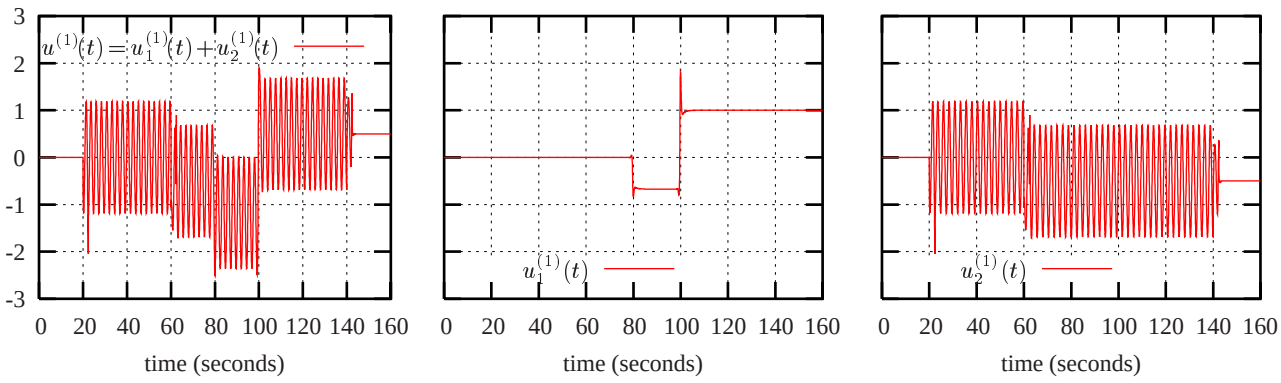

Figure 1: A simple example: control signal for plant input 1 (left). *It is computed by the* R-GPC *controller as* $u^{(1)}(t) = u_1^{(1)}(t) + u_2^{(1)}(t)$. *The middle part details the contribution of* $u^{(1)}(t)$ *to reference tracking, the right one to disturbance rejection. (same vertical scale).*

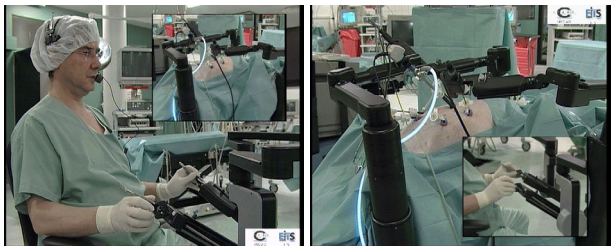

Figure 4: Laparoscopic robotic system at work (IRCAD, Strasbourg). *The* AESOP *robot is the endoscope positioner*.

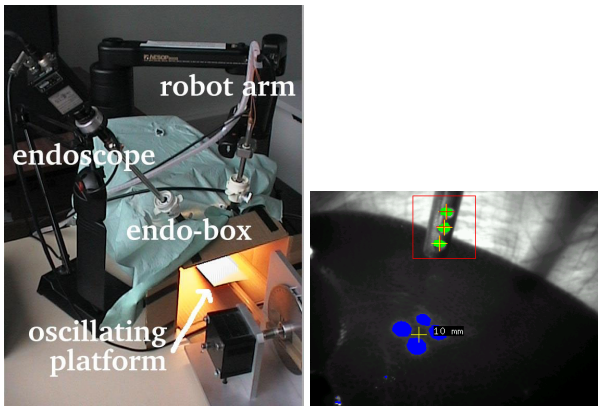

Figure 5: System setup. (a) left: The organ motion is simulated thanks to an oscillating plate. *The robot is an* AESOP *surgical arm holding a laser-pointing instrument.* (b) right: *In-vivo* snapshots with distance estimation from the instrument's tip to the organ using optical marks.

namics of the first joint that is responsible for the translation of the tool along its axis. Its transfer function is identified using Matlab® as:

$$F(z^{-1}) = \frac{0.01606z^{-d}}{1 - 1.7606z^{-1} + 0.9242z^{-2} - 0.1636z^{-3}}$$

with $d = 7$ and the sampling period is $T_e = 0.040\,s$.

3.1 Simulation on a laboratory test-bed

The R-GPC controlled system is first tested in a laboratory experimental setup with use of the endoscopy-training box that is shown in Fig. 5a: the endoscope is a monochrome PAL camera mounted on a static holder; images from the box are updated every $T_e = 40\,ms$. The plate shown in the endo-box is made oscillating (with a period T^*) thanks to an oscillating platform whose cyclic trajectory is precisely controlled by a one degree of freedom robot. The robot arm is holding a laser pointing instrument equipped with optical marks for distance estimation (see Fig. 5b, [3]). Measurements are fed into the predictive controller, which, in turn, returns the optimal speed to be applied along the instrument's axis. The vision thread and the predictive control thread are hosted by a 1700 MHz bi-processor PC computer running Linux that communicates with the surgical robot via a serial link. Controller computations are synchronized with the image acquisition.

The system setup and its visual servoing loop are summarized in Fig. 6. Predictions are made using the robot model and current and past outputs and control inputs. Command $u_1(t)$ is computed according to the finite receding horizon strategy so as to ensure an optimal tracking of the reference depth $r(t)$ in the future. Command $u_2(t)$ is computed according to the disturbance period T^* in order to cancel the effect of the oscillating plate. Command $u(t) = u_1(t) + u_2(t)$ is sent to the robot and controls the depth $y(t)$ of the instrument.

Movement of the oscillating plate is set so that $T^* = 2.4\,s$ and the oscillations yield cyclic depth disturbances whose amplitude is about $6\,mm$. Controller parameters are set to $N_1 = 8$, $N_2 = 45$, $N_u = 30$, $\lambda = 0.55$ and $\mu = 0.70$.

A classical GPC controller with the same parameters (except that λ is not considered) and no periodic signal generator is first used in Figure 7 where the reference is kept to a constant distance. The perturbation is badly attenuated (residual ampli-

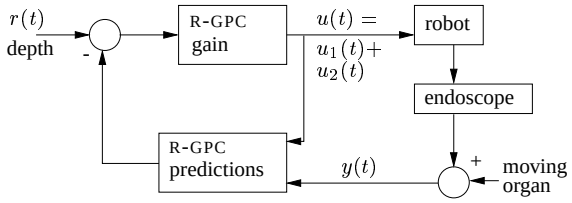

Figure 6: Block-diagram of the predictive control system. *Instrument's depth $y(t)$ is measured in the endoscope images and is controlled by visual servoing, using references $r(t)$.*

tude is $4\,mm$) and makes the system ouput vary periodically with time.

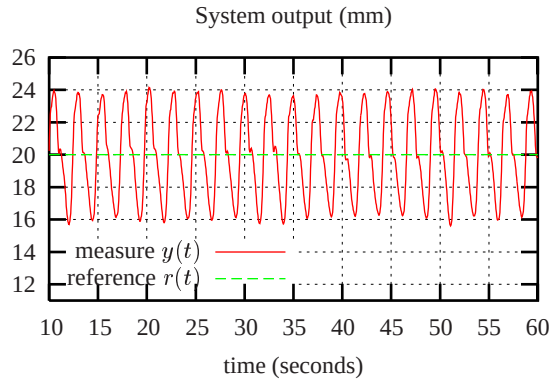

Figure 7: System output with a classical GPC and repetitive disturbances.

Figure 8 shows the system response as it is driven by the R-GPC controller with varying references. Effect of the disturbance is clearly reduced and the residual error has an amplitude of about $1.5\,mm$.

The corresponding command $u(t)$ and its two components $u_1(t)$ and $u_2(t)$ are shown in Fig. 9. Curve for $u_1(t)$ is shown to be in accordance with reference changes whereas $u_2(t)$ is made oscillating for reducing the disturbance amplitude.

3.2 *In-vivo* results

The experiment is now run in *in-vivo* conditions on a living pig at the operating room of IRCAD. Figure 10 depicts the control curves obtained for a reference of $9\,mm$ and periodic disturbances due to breathing. Curves are shown to be comparable to the ones in Fig. 9. Note that the amplitude modulation of component u_2 is due to the movement of the endoscope's insertion point into the breathing pig.

4 Conclusion

This paper presented a repetitive model predictive controller applied to the problem of tracking periodic motions induced by respiration in laparoscopic robotized teleoperations. The periodic property of the disturbance has been included into the input-output model of the controlled system so as to anticipate perturbating motions. A new cost function has been presented for the unconstrained generalized predictive controller where separate contributions of the control output to reference tracking and to disturbance rejection are computed. This formulation ensures the robot can follow a time-varying reference and track periodic output disturbances, both simultaneously and in an independent manner. Experimental results have been shown for visually servoing the insertion depth of a surgical tool in an endoscopic operation with an AESOP surgical robotic arm.

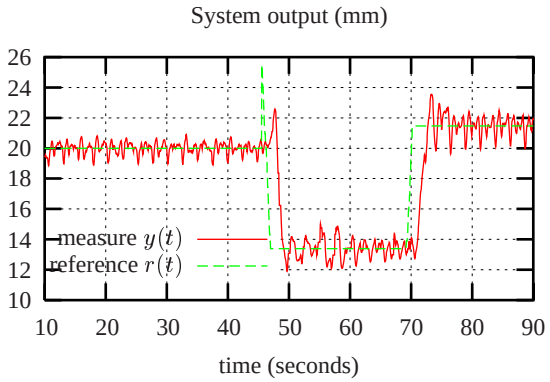

Figure 8: System output with a varying reference.

5 Acknowledgements

The authors thank Computer Motion Inc. that has graciously provided the AESOP medical robot.

References

[1] E. F. Camacho and C. Bordons. *Model Predictive Control*. Springer-Verlag, London, 1999.

[2] D. W. Clarke, C. Mohtadi, and P. S. Tuffs. Generalized predictive control - part. 1: The basic algorithm. *Automatica*, 23:137–160, 1987.

[3] A. Krupa, C. Doignon, J. Gangloff, and M. de Mathelin. Combined image-based and depth visual servoing applied to robotized laparoscopic surgery. In *Proc. of the 2002 IEEE/RSJ International Conference on Intelligent Robots and Systems*, Lausanne, Switzerland, October 2002.

[4] J. H. Lee, S. Natarajan, and K. S. Lee. A model-based predictive control approach to repetitive control of continuous processes with periodic operations. *Journal of Process Control*, (11):195–207, 2001.

[5] S. Natarajan and J. H. Lee. Repetitive model predictive control applied to a simulated moving bed chromatography system. *Computers and Chemical Engineering*, (24):1127–1133, 2000.

[6] M. Steinbuch. Repetitive control for systems with uncertain period-time. *Automatica*, 38:2103–2109, 2002.

[7] G.-Y. Zhu, A. Zamamiri, M. A. Henson, and M. A. Hjortsø. Model predictive control of continuous yeast bioreactors using cell population balance models. *Chemical Engineering Science*, (55):6155–6167, 2000.

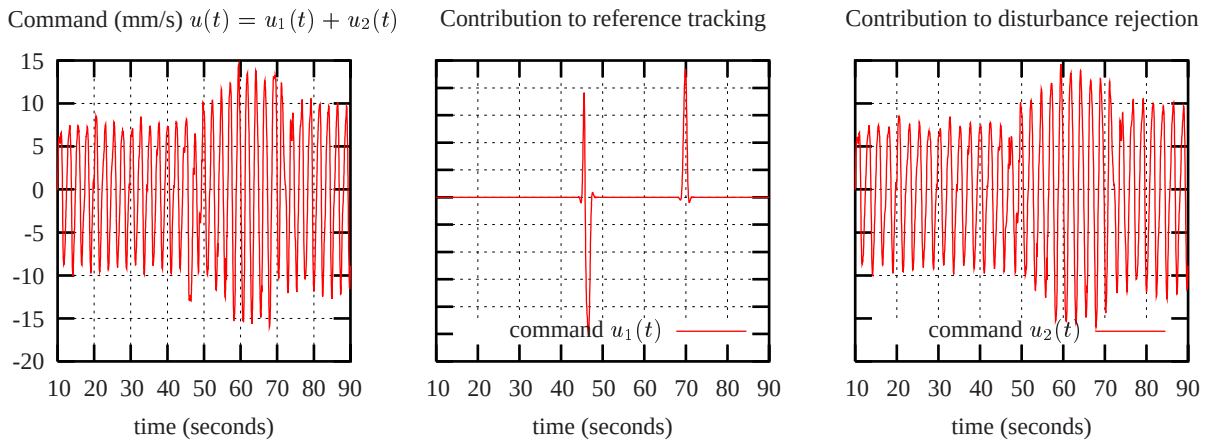

Figure 9: System command for Fig. 8. *The system is driven to the varying reference as shown by command $u_1(t)$ (middle). Term $u_2(t)$ reflects the controller behaviour for disturbance rejection (right).*

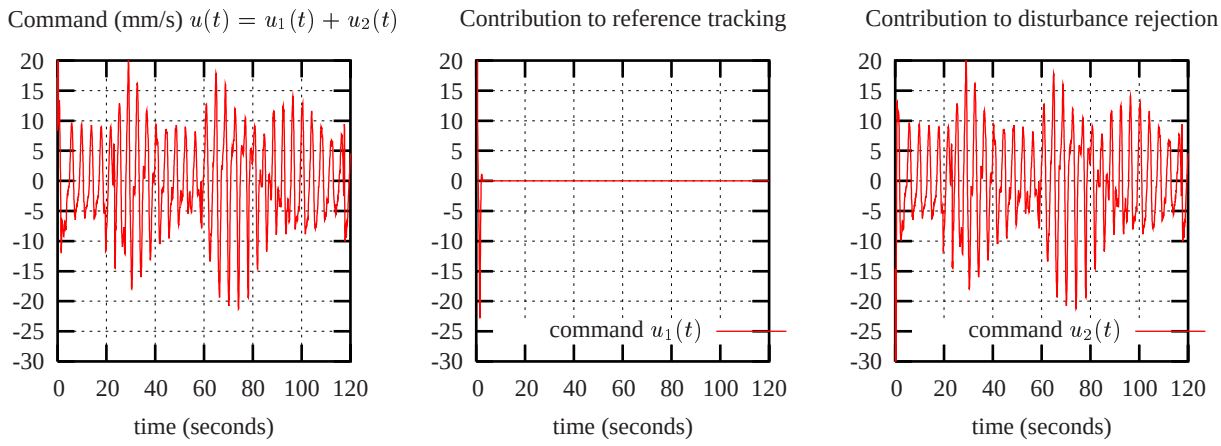

Figure 10: Robot control input in *in-vivo* conditions. *The system is driven to a constant reference of $9\,mm$ (see transient for $u_1(t)$, middle). Term $u_2(t)$ reflects the controller behaviour for disturbance rejection (right).*